

Modified pulsar current analysis: probing magnetic field evolution

A.P. Igoshev^{1*}, S.B. Popov²

¹ *Department of Astrophysics/IMAPP Radboud University Nijmegen P.O. Box 9010 6500 GL Nijmegen The Netherlands*

² *Sternberg Astronomical Institute, Lomonosov Moscow State University, Universitetsky prospekt 13, 119991, Moscow, Russia*

Accepted — Received —

ABSTRACT

We use a modified pulsar current analysis to study magnetic field decay in radio pulsars. In our approach we analyse the flow, not along the spin period axis as has been performed in previous studies, but study the flow along the direction of growing characteristic age, $\tau = P/(2\dot{P})$. We perform extensive tests of the method and find that in most of the cases it is able to uncover non-negligible magnetic field decay (more than a few tens of per cent during the studied range of ages) in normal radio pulsars for realistic initial properties of neutron stars. However, precise determination of the magnetic field decay timescale is not possible at present. The estimated timescale may differ by a factor of few for different sets of initial distributions of neutron star parameters. In addition, some combinations of initial distributions and/or selection effects can also mimic enhanced field decay. We apply our method to the observed sample of radio pulsars at distances < 10 kpc in the range of characteristic ages $8 \times 10^4 < \tau < 10^6$ years where, according to our study, selection effects are minimized. By analysing pulsars in the Parkes Multibeam and Swinburne surveys we find that, in this range, the field decays roughly by a factor of two. With an exponential fit this corresponds to the decay time scale $\sim 4 \times 10^5$ yrs. With larger statistics and better knowledge of the initial distribution of spin periods and magnetic field strength, this method can be a powerful tool to probe magnetic field decay in neutron stars.

Key words: magnetic fields – stars: neutron – pulsars: general – methods: data analysis – methods: statistical.

1 INTRODUCTION

The pulsar current analysis is a known method to study the evolution of radio pulsars. It was originally proposed and applied by Vivekanand & Narayan (1981) and Phinney & Blandford (1981a), and more recently revised by Vranešević & Melrose (2011). It is assumed that pulsars are born in a certain region (or regions) in the spin period — period derivative ($P - \dot{P}$) plane, and then they move along evolutionary tracks (which depend on the magnetic field evolution model), until they finally disappear in another part of the $P - \dot{P}$ diagram. The classical pulsar current evolves according to a kinetic equation with a source term (see Vranešević & Melrose 2011 for details). One of the main results of this technique is an estimate of a total birthrate. In addition, information about initial spin period distribution can be uncovered by this method. For example, this technique provided evidence in favour of so-called “injection” in the pulsar current at $P \sim 0.5$ s (Vivekanand & Narayan 1981, although this result has been questioned in later studies, see Vranešević & Melrose 2011).

In this article we propose a modification to the pulsar current analysis. The main difference from the standard technique is that we look at the pulsar current along the spin-down age, τ , direction

(black arrow in Fig. 1) instead of the spin period axis. This approach has an advantage with respect to the standard pulsar current analysis: if the magnetic field of a neutron star rapidly decays, then the spin period grows very slowly. However, the characteristic age continues to grow. This can be used to probe field decay in neutron stars.

The problem of magnetic field decay in neutron stars is a long standing one (see an early discussion in Ostriker & Gunn 1969 and recent theoretical analysis in Geppert 2006; Cumming et al. 2004). Different kinds of analysis have been used to probe the field evolution. Most often the population synthesis approach was used to study the whole population of radio pulsars, and controversial conclusions were reported. Bhattacharya et al. (1992) made an important claim that there is no significant field decay during pulsar lifetime. Recently, Faucher-Giguère & Kaspi (2006) also concluded that the decay is not necessary to describe the observed population of radio pulsars. Oppositely, Gonthier et al. (2002) presented arguments in favour of a decaying field. Popov et al. (2010) presented a model in which several populations of neutron stars (magnetars, cooling near-by neutron stars, and radio pulsars) have been explained within the framework of a unique model of magneto-rotational evolution. However, for ordinary radio pulsars the effect of field decay is not very pronounced, and so it is difficult to un-

* E-mail: ignotur@gmail.com;

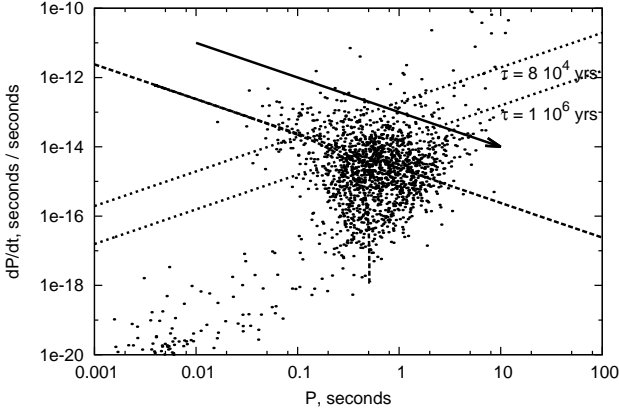


Figure 1. $P - \dot{P}$ diagram. Black dots represent normal pulsars from the ATNF catalogue. With dashed lines we show two evolutionary tracks: with constant and with an exponentially decaying field. Dotted lines correspond to two values of τ . Finally, the solid arrow (corresponding to the gradient of characteristic age) illustrates the direction in which τ is growing. In our approach we study pulsar current along this direction.

cover it. Studies of Be/X-ray binaries have generally confirmed this model (Chashkina & Popov 2012).

Magnetic field decay can be highly non-uniform during the lifetime of a neutron star. Thus analysis of the field evolution over a relatively long time interval can be, in some sense, misleading. On one hand, it is very important to put constraints on the very long timescale evolution of the field. In the near future this can be done on a time scale of billions years, for example, if old isolated neutron stars accreting from the interstellar medium are discovered (Konenkov & Popov 1997; Popov & Prokhorov 2000; Boldin & Popov 2010). On another hand, it is useful to analyse field evolution at different – even relatively short – periods of time. In this paper we study the magnetic field evolution of normal radio pulsars with ages $\sim 10^5 - 10^6$ yrs.

We employ our method to estimate the magnetic field decay timescale. We then test the method with samples of synthetic pulsars generated with a population synthesis code, and discuss different caveats that may be encountered during the analysis. Finally, we apply our method to large samples of known pulsars. Some preliminary results of this study have been reported by Igoshev et al. (2014).

The article is organized as follows. In the next section we describe the main aspects of the pulsar current analysis and discuss our methodology. In Section 3 we briefly summarize basic properties of the population synthesis code which was used to generate synthetic samples of pulsars, and then we apply these samples to test our method of field decay reconstruction. After that, in Sec. 3.2, we study the influence of the source term. Our main results on field decay in observed radio pulsars are presented in Section 4. In Section 5 we discuss uncertainties of the method and, finally, present our conclusions in the last section.

2 MODIFIED PULSAR CURRENT ANALYSIS

As in the classical pulsar current analysis (Vivekanand & Narayan 1981; Phinney & Blandford 1981a), we assume that the law describing the time evolution of the magnetic field is the same for all pulsars and can be written as $B(t) = B_0 f(t)$, where B_0 is the initial magnetic field (which can be different for each pulsar) and

$f(t)$ is the decay function, which might be interpreted as a statistical average of the real field evolution of individual pulsars. Our goal is to reconstruct $f(t)$ from an observational sample of pulsars with measured spin period, P , and period derivative, \dot{P} . Note that this approach is independent of the physical mechanism causing the magnetic field evolution. It simply provides a purely phenomenological fit to the decay function.

We begin with the following general expression for the magneto-dipole braking (Philippov et al. 2014):

$$P\dot{P} = \beta(\kappa_0 + \kappa_1 \sin^2 \chi)B^2, \quad (1)$$

where $\beta = (\pi^2 R^6)/(Ic^3)$, I is the moment of inertia, R is the neutron star radius, $B \equiv B(t)$ is the magnetic field strength at the magnetic pole, c is the speed of light, and χ is the angle between the magnetic axis and the spin axis. Note that $B(t)$ is a function of time.

The values of the coefficients κ_0 and κ_1 determine the magnetospheric torque. The most recent 3D simulations for vacuum, force-free, and resistive magnetospheres (Philippov et al. 2014) show that these coefficients are ≈ 1 for a variety of magnetospheric models. The classical magneto-dipolar radiation formula in vacuum is recovered with $\kappa_0 = 0$ and $\kappa_1 = 2/3$ (Ostriker & Gunn 1969). In this case a neutron star experiences a very rapid alignment of the rotation and magnetic axis (see, for example, Eliseeva et al. 2006); in contradiction with observations. Other alternatives to the magneto-dipole formula (see, for example, Gurevich et al. 1993; Beskin et al. 2013 and references therein) are also similar to Eq.(1), but with a different numerical prefactor or/and different dependence on the angle, χ . For our purposes in this paper, a particular choice of the coefficients is not important. Hereafter we assume that $\kappa_0 = \kappa_1 = 1$, and that the evolution of the angle χ is not relevant on the timescales we are interested in (this was checked in a recent study by Gullón et al. 2014). Therefore, $\sin^2 \chi = \text{const}$, and for simplicity we assume everywhere below that $\sin^2 \chi = 1$.

We treat Eq.(1) as a differential equation, and we combine its solution with the standard definition of the spin-down age: $\tau = P/(2\dot{P})$. We then obtain:

$$\tau(t) = \frac{\beta \int_0^t B^2(\tau') d\tau' + 0.25 P_0^2}{\beta B^2(t)}. \quad (2)$$

We formally average this equation over distributions of initial periods and magnetic fields (see Appendix A for details):

$$\begin{aligned} \overline{\tau(t)}|_{P_0, B_0} &= \frac{\int_0^t \overline{f^2(\tau')} d\tau'}{\overline{f^2(t)}} + \frac{\overline{P_0^2}}{4\beta \overline{B_0^2} \overline{f^2(t)}} = \\ &= \frac{1}{\overline{f^2(t)}} \left(\int_0^t \overline{f^2(\tau')} d\tau' + \frac{\overline{P_0^2}}{4\beta \overline{B_0^2}} \right), \end{aligned} \quad (3)$$

where $\overline{P_0^2}/(4\beta \overline{B_0^2})$ may be considered as an averaged initial spin-down age. This value can be also understood as the median initial spin-down age: half of pulsars have their initial spin-down ages smaller than $\overline{\tau_0}$.

Then we differentiate Eq. (3) by t and obtain:

$$\frac{\dot{f}(t)}{f(t)} = -\frac{\dot{\tau}(t)}{2\tau(t)} + \frac{1}{2\tau(t)}. \quad (4)$$

In Eq.(4) and below (unless the opposite is directly stated) we do not use overline notation for characteristic ages, as effectively in our method we always deal, not with the τ of individual, pulsars but with some smoothed or average values. It is remarkable that the

form of the differential equation does not depend on the averaged initial spin-down age.

After we integrate Eq.(4), we obtain:

$$f(t) = \exp\left(\int_{\tau_{\min}}^t \frac{dt'}{2\tau(t')}\right) / \sqrt{\tau(t)/\tau_{\min}}, \quad (5)$$

where the value τ_{\min} corresponds to the lower boundary of the range of characteristic ages that we use in our analysis. Thus, the problem is reduced to finding a reasonable approximation to the function $\tau(t)$, from which the field evolution function $f(t)$ can be recovered by numerical integration of Eq. (5). This can be done using the kinetic equation already used to study the $P - \dot{P}$ distribution of radio pulsars (Beskin et al. 1986; Phinney & Blandford 1981b; Deshpande et al. 1995).

Let us consider a two-dimensional space with the true age, t , as the time coordinate, and τ playing the role of the space coordinate. Let $n(\tau, t)$ be the pulsar distribution function in this space. This is the number of pulsars with spin-down age from τ to $\tau + d\tau$ and true age from t to $t + dt$. We can write the following continuity equation for the pulsar evolution:

$$\frac{\partial n}{\partial t} + \frac{\partial}{\partial \tau} \left(n \frac{d\tau}{dt} \right) = U - V. \quad (6)$$

Here U and V are source terms describing the rates of birth and death of pulsars (latter does not necessary imply some switching-off mechanism; old pulsars can simply become too faint or too narrow-beamed so we cannot detect them anymore). Furthermore, we assume that during a typical period of a pulsar's activity, the whole ensemble of sources is in dynamical equilibrium and therefore we may neglect the time variations of pulsar distributions and search for stationary solutions. The second (and the strongest) assumption is that both source terms can be neglected in some range of characteristic ages $[\tau_{\min}, \tau_{\max}]$ (see Sec. 2.1), and here Eq. (6) simply reduces to:

$$\frac{\partial}{\partial \tau} \left(n \frac{d\tau}{dt} \right) = 0. \quad (7)$$

Note that the distribution of spin-down ages $n(\tau)$ can be written as:

$$n(\tau) = \frac{\Delta N}{\Delta \tau} = \frac{\Delta N}{\Delta t} \frac{\Delta t}{\Delta \tau}. \quad (8)$$

In the limit of infinitesimal intervals and for a constant birth-rate (represented by n_{br}) the equation above takes the form:

$$n(\tau) = n_{\text{br}} \frac{dt}{d\tau}. \quad (9)$$

Then we integrate this equation to get the cumulative distribution¹:

$$N(\tau) \equiv \int_0^{\tau} n(\tau', t) d\tau' = n_{\text{br}} t(\tau). \quad (10)$$

If we assume that the magnetic field remains constant up to some characteristic age τ_{\min} , we obtain $\tau = t + \bar{\tau}_0$ for $\tau < \tau_{\min}$. Therefore:

$$n_{\text{br}} = \frac{N(\tau_{\min})}{\tau_{\min} - \bar{\tau}_0} \approx \frac{N(\tau_{\min})}{\tau_{\min}}. \quad (11)$$

¹ The method to reconstruct the field evolution function is realized as a computer code "Spin Down Ages" (SDA), available on-line at <http://www.pulsars.info/decay.html>

If $\tau > \tau_{\min}$ then a statistical estimate of the true age of radio pulsars can be defined as:

$$t_{\text{stat}}(\tau) \equiv \frac{N(\tau)}{n_{\text{br}}}. \quad (12)$$

If we invert this expression and substitute the result into Eq. (5) to perform numerical integration, we can reconstruct the decay function, $f(t)$. To do this in a systematic manner, we first introduce a logarithmic grid for spin-down ages and find the cumulative distribution of τ . This is a binned distribution, which is subjected to significant fluctuations. It is useful to replace this distribution by a smoothed one applying a linear filter (sliding mean in a window). This filter is determined by the parameter r_s which is the size of the window. Explicitly:

$$n'_k = \frac{1}{r_s} \sum_{i=-(r_s-1)/2}^{(r_s-1)/2} n_{k+i}. \quad (13)$$

Here n'_k is the number of pulsars in the k th bin after filtering, and n_{k+i} — the number of pulsars in the $k+i$ th bin before filtering.

Finally, we apply the method only in a relatively narrow range of spin-down ages $[\tau_{\min}, \tau_{\max}]$. At large values of τ , different selection effects can be important, and to get rid of them we define an upper boundary to the spin-down age. At small values of τ initial parameters of a pulsar can dominate. We assume that τ can be represented as a sum of two values: one related to evolution and another to the initial parameters. As initial parameters are unknown we use a procedure of averaging over them (see Appendix A), and select τ_{\min} in such a way as to minimize the effect of the initial parameters. Details of the choice of τ_{\min} and τ_{\max} are given in the next subsection.

2.1 Determination of τ_{\min} and τ_{\max}

The choice of these boundaries is determined by the necessity to avoid selection effects. Our method has two natural limitations, which do not allow us to apply it to very young or very old pulsars. First, we assume that pulsars are born with $\tau < \tau_{\min}$. However, in reality some objects can have initially $\tau > \tau_{\min}$, and for them we cannot distinguish between field decay and large τ_0 (Igoshev & Popov 2013). This is one of the sources of uncertainty in our approach. The second assumption is that there is no selection against older pulsars within the range. However, older pulsars are usually weaker and cannot be detected at large distances from the Sun. It leads to the leakage of aged pulsars closer to the right boundary of the range. Let us discuss both limitations in more details.

To choose the left boundary of the range we want to guarantee for most of the pulsars in a sample that τ_{\min} is larger than $\text{few} \times \bar{\tau}_0$ (see Eq.3). The definition of the averaged spin-down age determined by Eq. (3) includes the average initial spin-down age. While the first term in the right hand side in parentheses contains all the field evolution, the second one is just some additional constant. To estimate this term we use the following values: $P_0 = 0.3$ s, $B = 4 \times 10^{12}$ G, and $\beta = 1.6 \times 10^{-39}$ G⁻² s:

$$\bar{\tau}_0 = \frac{P_0^2}{4\beta B_0^2} \approx 2.8 \times 10^4 \text{ yrs}. \quad (14)$$

So, $\bar{\tau}|_{B_0, P_0} \sim \tau$ (without additional terms) for relatively old pulsars with ages significantly larger than the one estimated above. Consequently, our method may be safely applied to pulsars with spin-down ages larger than $\tau_{\min} \sim 8 \times 10^4$ years. To make an

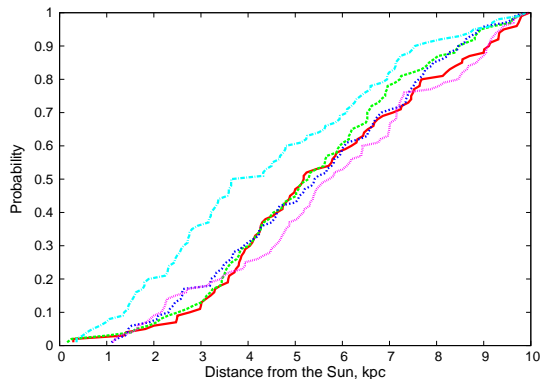


Figure 2. Cumulative distance distributions of pulsars. Red solid line – $\tau \in [700, 1.2 \times 10^5]$ years; green dashed line – $\tau \in [1.2 \times 10^5, 4.5 \times 10^5]$ years; blue short-dashed line – $\tau \in [4.5 \times 10^5, 9.6 \times 10^5]$ years; violet dotted line – $\tau \in [9.6 \times 10^5, 1.6 \times 10^6]$ years; and light blue dashed and dotted line – $\tau \in [4 \times 10^6, 6 \times 10^6]$ years. Each age interval contains 100 pulsars. In this figure we plot all normal pulsars from the ATNF pulsar catalogue (Manchester et al. 2005), excluding those in binaries or in globular clusters. (Color on-line.)

estimate of Eq.(14), we choose values such that according to plots in Popov & Turolla (2012) most of pulsars have $P_0 < 0.3$ s and $B_0 > 4 \times 10^{12}$ G, i.e. they are born out of the range under study.

To choose the right boundary of the range for the real sample (i.e., for a sample of observed pulsars) we use the following procedure to probe the leakage of aged pulsars. Weak pulsars can be hardly ever detected at large distances from the Sun. Therefore, shapes of radial distribution functions for young and old pulsars are different because it is not possible to detect weak, aged pulsars with the same efficiency at all distances, vice versa, till shapes of radial distribution functions for pulsars of different ages are similar (i.e., until the difference can be explained by random fluctuations) the leakage of old pulsars can be neglected. We illustrate this in Fig. 2.

It is seen that for ages 700 — 10^6 yrs the radial distribution functions have similar shapes (this is also confirmed by the Kolmogorov-Smirnov test). However, pulsars with spin-down ages $4 \times 10^6 - 6 \times 10^6$ years have a radial distribution function with a significantly different shape: there are more pulsars at small distances than in younger groups. This is because some distant, aged pulsars avoid detection due to their weakness, so there is a leakage of these sources which can mimic field decay. To avoid this, we limit our sample to $\tau = 10^6$ yrs. This value is a bit flexible and potentially can be increased, but to be conservative we prefer not to do so.

The similarity of radial distributions might be not sufficient, because even if these distributions are alike for different age groups, some other selection effects which do not influence the radial distribution can be significant. Nevertheless, this similarity is a necessary condition because any variation of the number of pulsars with age due to selection effects, mimic field evolution.

3 POPULATION SYNTHESIS AND TESTS

Population synthesis is a numerical method for studying large samples of evolving objects (Popov & Prokhorov 2007). Its most popular variant (which we apply here) is based on Monte-Carlo procedures which use some initial properties and evolution laws for individual sources. Compellingly, selection effects can also be mod-

Table 1. Results of the SDA code for the synthetic models. τ_d corresponds to the timescale used in the numerical model, while τ_{SDA} and τ_{hist} are the ones obtained by applying the SDA code and a direct fit of $N(\tau)$.

Name	$\log \mu_{B_0}$ [G]	$\log \sigma_{B_0}$ [G]	μ_{P_0} [s]	σ_{P_0} [s]	α	τ_D [Myr]	τ_{SDA} [Myr]
A1	12.60	0.47	0.33	0.23	0.50	∞	∞
A2	12.95	0.55	0.30	0.15	0.50	∞	10
B1	12.60	0.47	0.33	0.23	0.50	0.5	1.00
B2	12.95	0.55	0.30	0.15	0.50	0.5	0.690
C1	12.60	0.47	0.33	0.23	0.50	1	1.15
C2	12.95	0.55	0.30	0.15	0.50	1	0.560
D1	12.60	0.47	0.33	0.23	0.50	5	2.00
D2	12.95	0.55	0.30	0.15	0.50	5	0.80
E	13.04	0.55	0.22	0.32	0.44	~ 0.8	0.880

elled. As a result, we create a synthetic sample. Comparison between the observed and simulated samples can be done in order to infer properties of the population.

3.1 Tests with synthetic samples

The best approach to check the quality of our method is to use a set of synthetic samples, generated by a robust population synthesis code, with several different sets of initial conditions, with and without field decay, which can more or less successfully reproduce the real sample of radio pulsars. For this purpose we use synthetic samples calculated (and provided to us) by Gullón et al. Detailed description of their code can be found in Gullón et al. (2014) and references therein. Below, we present the most essential details related to the population synthesis code.

Initial parameters of neutron stars such as period, magnetic field, position in the Galaxy, and kick velocity are randomly chosen according to some specified distributions. The distributions of initial magnetic fields (in log-scale) and periods are taken in the form of a Gaussian. The mean value and standard deviation vary depending on the model of evolution of the magnetic field (each model is fitted to reproduce the observed sample of pulsars). The considered values can be found in Table 1. The evolution of a pulsar spin period is calculated according to Spitkovsky (2006) i.e. $\kappa_0 = \kappa_1 = 1$ in Eq.(1) The magnetic inclination angle, χ , is uniformly chosen on the sphere, so its direction is isotropic. Evolution of the magnetic field with time, $B(t)$, characterizes each model we use (see Table 1). Finally, selection effects are taken into account. They determine the fraction of detectable sources among the generated pulsars. The radio luminosity depends on the spin period and its derivative. A popular form for this quantity is used (see, for example, Faucher-Giguère & Kaspi 2006):

$$\log L_{\text{rad}} = \log[L_0(P^{-3}\dot{P}_{-15})^\alpha] + L_{\text{corr}}, \quad (15)$$

where $\dot{P}_{-15} = \dot{P}/10^{15}$, $L_0 = 0.18$ mJy kpc² and L_{corr} is chosen randomly from a Gaussian distribution with zero average and $\sigma = 0.8$. The value of α can vary for different models the magnetic field evolution (see Table 1).

The synthetic samples are created with the following models of evolution of the magnetic field:

- Model A. No magnetic field decay: $f(t) = 1$.
- Models B, C, and D. Exponential decay: $f(t) = \exp(-t/\tau_D)$.
- Model E. A realistic law of field decay based on microphysical calculations.

Models A-D correspond to simplified scenarios, while the last one (E) represents a more advanced case. Model E corresponds to a realistic magneto-rotational and thermal evolution of neutron stars (see Viganò et al. 2013 and references therein), that was found to fit well the observational data on radio pulsars (Gullón et al. 2014). The Galactic pulsar birth rate in Model E is ~ 2 neutron stars per century. In this model the quadratic deviation of the atomic number in the pasta phase is taken to be $Q_{\text{imp}} = 25$, as is favoured by a recent study by Viganò et al. (2013). Other parameters are given in Table 1. Note, that in Models A-D, the law of field decay is unique for all pulsars. For Model E this is not the case. In this model pulsars with different initial parameters follow slightly different paths of field evolution.

The initial parameters for all models are listed in Table 1. We use two different sets (labeled as 1 and 2) for the first four models (A-D). They are defined by $\log \mu_{B_0}$, $\log \sigma_{B_0}$, μ_{P_0} , σ_{P_0} , α (see Table 1). For Model E a different set of initial parameters (that seems to fit better the observational data, see Viganò et al. 2013) was used.

Since the population synthesis code generates samples with pre-defined magnetic field decay law, analysis of the results and detection of errors are clear. Errors are divided into random and systematic. Former ones appear because of the discreteness of the pulsar ensemble; while the latter are due to the intrinsic limitations of the method. For each model we have generated a sample of 10000 sources. The results of our tests are presented in Table 1 and Fig. 3.

The following notes can be made:

- The method is sensitive to the magnetic field decay: the obtained timescales systematically increase for models with slower decay (being maximal for model A).
- Derived decay timescales in the cases of models B1 and C1 are similar. The same is true for samples B2 and C2. However, the actual values of τ_D used to generate each sample in these pairs differ by a factor 2.
- With both methods, when we use the second set of initial parameters (A2, B2, C2, D2) the derived time scales are always smaller.

3.2 Influence of the source term

The last item of the previous subsection implies that we have some systematics which results in a more rapid decay if the initial distribution of characteristic ages is narrower. To analyse this, we perform simple calculations with a toy-model population synthesis.

We consider consequent populations of pulsars born with the same initial distributions with a time step Δt . In Fig. 4 we plot distribution of initial characteristic ages for sets 1 (used for models A1, B1, ...) and 2 (A2, B2, ...). Note, that for the second set the distribution is narrower (data are normalized in such a way that the areas below both curves are equal, and the peak of the second set at low initial characteristic ages is compensated by larger number of pulsars with initial characteristic ages $> 10^5$ yrs in the first set, which is barely visible in the plot).

If there is no field decay, then the distribution of characteristic ages for a single generation of pulsars is just shifted along the age axis. So the total distribution for all generations would be formed by a number of peaks separated by Δt , each of which corresponds to one generation of pulsars. However, the height of each peaks would be different because, in the total distribution at each characteristic age there is a contribution from younger generations. So, peaks which correspond to older generations will be systematically higher. Then the cumulative distribution of characteristic

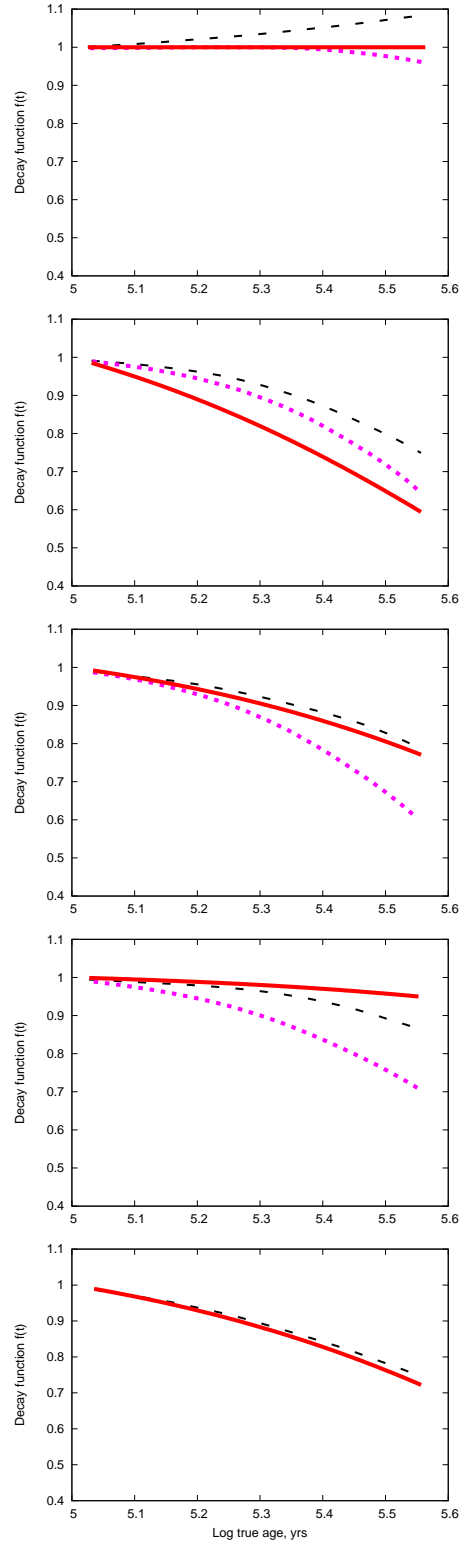


Figure 3. The field decay reconstruction for models A-E (from top to bottom). In each plot a solid line shows the actual decay law used to generate the synthetic sample (except the bottom plot where the solid line is an average magnetic field decay law, as there the law was not unique for all pulsars). Dashed lines correspond to the first set of initial conditions (models A1, B1, ...). Dotted lines are plotted for decay reconstruction in which the second set was used (models A2, B2, ...). For model E (bottom plot) only one set of parameters have been used, so just one reconstructed curve is presented, and it is very close to the decay function used in calculations.

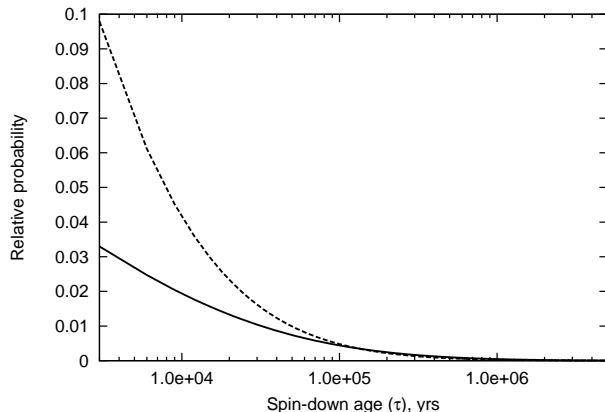


Figure 4. The PDF of the initial spin-down age. Solid and dashed lines are plotted for the first and second type of initial condition, correspondingly. Curves are normalized so that the areas below each of them are equal.

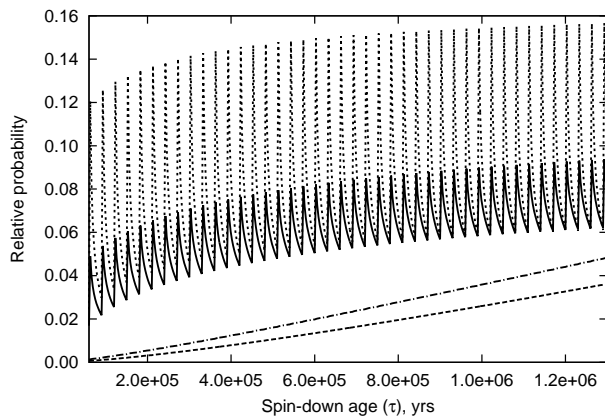


Figure 5. Results are obtained for constant magnetic field. Two upper sawtooth curves are PDFs of characteristic ages for several sequential generations of pulsars separated by $\Delta t = 30000$ years. Solid and dashed lines correspond to the 1st and the 2nd types of initial conditions, respectively. Lower dashed and dot-and-dashed lines are cumulative distribution functions of characteristic ages for the 1st and the 2nd type of initial conditions, respectively. For the vertical axis we use arbitrary units, so curves are shifted respect to each other to show their behaviour better.

ages is growing faster, and this function would have positive second derivative (Fig. 5). This effect explains why we, formally, obtained a growing magnetic field for model A1 (see Fig. 3, top plot).

If the field is decaying then the situation is different. At first, peaks corresponding to different generations would not be equidistant along the axis of characteristic ages (our analysis is based on this effect). Due to field decay older generations would have enhanced characteristic ages as period derivative of pulsars is rapidly decreasing (the characteristic age grows faster than the true age if the field decays: $\Delta\tau > \Delta t$).

In addition, there is another effect which we have not included into our analysis. Each peak is stretching due to decaying field, and so its height decreases (Fig. 6, middle curves). As we show below, due to this effect in some cases we overestimate the rate of field decay. As the result of growing distances between each sequential generations, the cumulative distribution has negative second derivative (Fig. 6, bottom curves).

Note that both effects — growing (due to contributions of

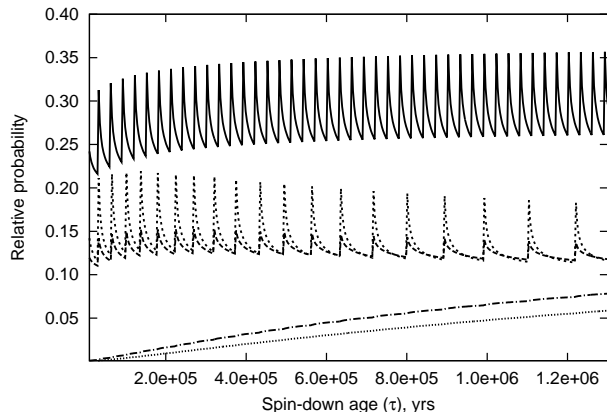


Figure 6. Three upper sawtooth curves are PDFs of characteristic ages for several sequential generations of pulsars separated by $\Delta t = 30000$ years. Solid line on top represents the same PDF as the solid line in Fig. 5. Dotted and dashed sawtooth curves are plotted for the case of decaying magnetic fields for the 2nd and the 1st type of initial conditions, respectively. Below we plot two cumulative distributions of characteristic age. The upper of them is for the 2nd set of initial conditions, and the lower one — for the 1st. For the vertical axis we use arbitrary units, so curves are shifted respect to each other to show their behaviour better.

younger generations) and stretching (due to field decay) of the peaks — are smaller than the effect of the growing separation between peaks because the number of pulsars with $\tau_0 > \bar{\tau}_0$ is less than a half of the total number (see Appendix B).

4 RESULTS. FIELD DECAY RECONSTRUCTION

The main goal of this study is to probe the field decay of real radio pulsars. We apply our methods to large observed samples of radio pulsars to study field decay in these objects. As we need to have as large statistics as possible, as well as uniform samples, we firstly place we study sources from the ATNF catalogue (Manchester et al. 2005). Then we apply our method to the largest uniform subsample of the ATNF — to the Parkes Multibeam and Swinburne surveys (hereafter PMSS) (Manchester et al. 2001). Besides the PMSS, the ATNF catalogue includes Jodrell B (Clifton & Lyne 1986), Green Bank Northern Hemisphere survey (Damashek et al. 1978), Princeton-NRAO survey (Dewey et al. 1985), Green Bank fast pulsars survey (Sayer et al. 1997), and other data. The PMSS is a significant (major) part of the ATNF pulsar catalogue. This is the largest relatively uniform sample of radio pulsars. We exclude sources not originally detected in radio surveys (like, magnetars, near-by cooling neutron stars, etc.) Also from both samples we exclude millisecond (recycled) pulsars, pulsars in globular clusters, and in binary systems. Finally, we use only sources closer than 10 kpc from the Sun. In total, we use 1391 objects from the ATNF, and 831 from the PMSS.

As before for synthetic samples (see Sec. 3) we reconstruct the magnetic field decay in the range of true (statistical) ages: $8 \times 10^4 < t < 3.5 \times 10^5$ yrs which corresponds to characteristic ages $8 \times 10^4 < \tau < 10^6$ yrs. Results are presented in Fig. 7.

The solid line shows the reconstruction for the PMSS data, and the dashed one for the ATNF. These two curves demonstrate very similar behaviour. The difference between them is less than 5 per cent. This supports the hypothesis that our results are weakly dependent on radio fluxes (for the selected range of characteris-

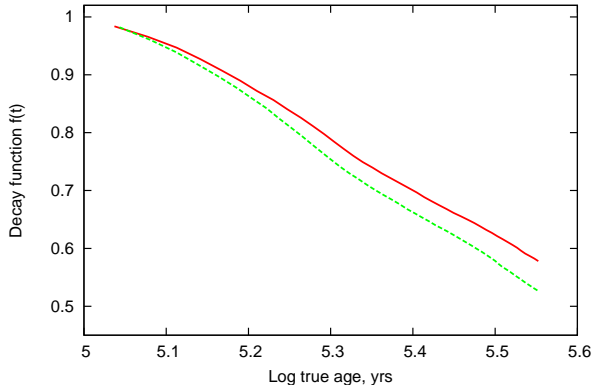


Figure 7. Field decay reconstruction for the ATNF (dashed line) and PMSS (solid line) samples. When fitted with an exponent, the time scale of decay is 0.38 Myrs for the ATNF sample, and 0.45 Myrs for the PMSS.

tic ages and distances). In addition, we see that an increase of the number of pulsars by a factor ~ 2 does not influence the results significantly. In Fig. 7 it can be seen visible that the field drops by a factor ~ 2 during the studied period of evolution. If we fit the derived decay by an exponent, then we obtain: $\tau_{\text{SDA}} = 0.38$ Myrs for the ATNF sample, and $\tau_{\text{SDA}} = 0.45$ Myrs for the PMSS sample. Interpretation of the results is beyond the scope of the paper, but it is tempting to note that the decay timescale is similar to the Hall decay in normal radio pulsars (Aguilera et al. 2008). Note, that we obtained $f(t)$ just for a limited range of τ . For larger ages the rate of field decay can be different, and our results cannot be extrapolated out of the studied range.

5 DISCUSSION

Results of our reconstruction of the magnetic field evolution can be influenced by several effects related to the assumptions we made. In this section we briefly discuss them.

In Eq. (6) we neglect both source terms. To satisfy this assumption we choose a lower boundary of the range of characteristic ages; τ_{min} (see Sec. 2.1). This choice is based on some assumptions about the initial parameters of neutron stars. If these assumptions are not valid, then the decay function is reconstructed with some systematic error.

If the initial distribution of characteristic ages is narrow then we can overestimate the rate of field decay. In reality, distributions of P_0 and B_0 can be wider than we use in our calculations. The fact that for the most realistic model, E, the reconstructed curves coincide well with the one used to produce the synthetic samples suggests that this is not a source of large error for the samples of observed pulsars.

In Appendix B we consider a mathematical model which helps to demonstrate the dependence of our results on initial distributions. This dependence appears to be relatively strong for the cases when $\tau_{\text{min}} \sim \bar{\tau}_0$, and weak when $\tau_{\text{min}} \gg \bar{\tau}_0$. Note, that if $\tau_{\text{min}} \sim \bar{\tau}_0$, then errors in the reconstruction of $f(t)$ will grow with increasing t . Therefore, as in the case of a real sample we do not know $\bar{\tau}_0$ with good precision, we have an additional reason to limit the considered range of t from above by only ($t \sim \text{few} \times \bar{\tau}_0$).

For the first set of initial conditions (A1, B1, ...) we can estimate that $\bar{\tau}_0 \approx 9 \times 10^4$ yrs $\approx \tau_{\text{min}}$. For the second set (A2, B2, ...) we have $\bar{\tau}_0 \approx 1.5 \times 10^4$ yrs $\approx \tau_{\text{min}}/5.5$. Finally, for the model E

the estimate is $\bar{\tau}_0 \approx 5 \times 10^3$ yrs $\approx \tau_{\text{min}}/15$. This explains why in the case of model E, the result of the field evolution reconstruction is in better agreement with the actual decay, than in the case of A1, B1, ...

When $\tau_{\text{min}} \sim \bar{\tau}_0$ the most important error in the reconstruction of $f(t)$ is related to the underestimation of the birthrate. This underestimate results in inadequate reconstruction of $t(\tau)$. Finally, the rate of field decay is underestimated (this is an analogue of the effect of summing up in Sec. 3.2).

If $\tau_{\text{min}} \sim 5\bar{\tau}_0$ then $n_{\text{br}} \approx C_1$ (see Appendix B1 for description of the coefficients C_k), and the main influence is due to other terms with coefficients C_2, C_3 , etc., which might give a smaller statistical age than the true age. This happens partly due to the effect that was illustrated in Sec. 3.2 as the stretching of peaks in the probability density function (PDF).

When we apply our method to observed samples (Sec. 4), we use $\bar{\tau}_0$ from Eq. (14) and $\tau_{\text{min}} = 8 \times 10^4$ yrs. Then $\tau_{\text{min}} \sim 3\bar{\tau}_0$, and we may overestimate the decay timescale by up to factor ≈ 2 . On the other hand, in Eq. (14) we used a rather conservative estimate of \bar{P}_0 . This value is not well known, and if it is smaller by a factor of a few ($\bar{P}_0 = 0.1$ instead of $\bar{P}_0 = 0.3$ sec, which would be in congruence with the results of Popov & Turolla 2012). In this case $\tau_{\text{min}} \sim 10\bar{\tau}_0$, and our estimates given in Sec.4 are robust.

Still other selection effects can influence the number of observable old pulsars. To ameliorate this we select an upper limit for the range of characteristic ages, τ_{max} . Still, potentially our results can be influenced by several effects. Let us discuss them.

On average, radio luminosity of older pulsars can be lower, so some may not be detected. We studied this possibility by checking the cumulative distance distributions of pulsars of different ages (Fig. 2). It seems that our choice of τ_{max} allows us to neglect the influence of this effect.

Neutron stars are known to be rapidly moving objects due to large kick velocities they obtain at birth (Lyne & Lorimer 1994). Older pulsars can avoid detection as they move out of the observable volume (for example, they can move out of the strip along the Galactic plane where most of the pulsar surveys are conducted). This would mimic field decay. Using numerical integration of pulsar motion in the Galactic potential we checked how many pulsars with ages $\sim 10^6$ yrs can leave the volume observed by the PMSS. This fraction is about a few per cent, and we conclude that this effect cannot influence our results significantly.

It is known that older pulsars can demonstrate nulling more often than younger sources (Rankin 1986). Then some pulsars may not be detected in surveys due to this effect, and again this can mimic field decay. However, the number of nulling pulsars is not large. Long observational time in each pointing allows modern surveys to detect even pulsars characterized by nulling with a duration of about a few minutes (McLaughlin et al. 2003), and we do not expect that this effect can significantly modify our conclusions.

By probing the magnetic field with P and \dot{P} , we always deal with the effective field, as the magnetic inclination angle is not known (see Eq. 1). If the inclination angle is also evolving, then it is very difficult to separate real magnetic field evolution from the angle evolution. However, recent studies (Gullón et al. 2014) demonstrate that the angle evolution in vacuum magnetosphere does not fit the data well — most pulsars align too fast. As for plasma-filled magnetospheres the study by Gullón et al. (2014) suggests that the data can be fitted well with the assumption of non-evolving angle (however, a fit with slightly evolving χ in the case of plasma-filled magnetosphere is also possible, see their Model B1). This allows

us to assume that the angle evolution can be neglected in the cases we study here.

Finally, in our approach we made an assumption of a unique law of magnetic field evolution for all neutron stars under study. Without doubt this is an oversimplification if one studies an ensemble of neutron stars. For example, extreme magnetars, or central compact objects in supernova remnants can have very different paths of magnetic field evolution. However, as we are interested only in normal radio pulsars in a particular range of ages, it seems reasonable to use in a first approximation the same law of field evolution for all sources.

6 CONCLUSIONS

We have proposed and developed a modification of the known pulsar current technique to reconstruct the magnetic field decay in an ensemble of radio pulsars based on spin-down age statistics.

We performed extensive numerical experiments to test our approach, and these revealed that in many cases, the deduced magnetic field decay law is robust, although obtained parameters are determined with some uncertainties.

We performed calculations for normal radio pulsars from the ATNF catalogue, and separately from the PMSS catalogue, with similar results. This demonstrates that the method is not particularly sensitive to the number of detected pulsars used in the analysis, and therefore, to the certain minimal detectable luminosity. Also it is found that the deduced magnetic field decay law could not be caused by random fluctuations or insufficient sensitivity of modern surveys.

By analysing pulsars in the ATNF, we find that in the range of characteristic ages $8 \times 10^4 < \tau < 10^6$ yrs (which corresponds to true ages $8 \times 10^4 < t < 3.5 \times 10^5$ yrs) the effective field decays by a factor ~ 2 . Taking into account recent results by Gullón et al. (2014), see above, we think that it is unlikely that all this decay of the effective field can be attributed to the evolution of magnetic inclination. We thus conclude that the dipole magnetic field indeed decays.

The reconstructed decay law is averaged over the entire studied pulsar population (exact rates of field decay can be different for different subpopulations among normal radio pulsars). The time scale of this decay, when fitted with an exponent, is about 4×10^5 yrs, which is similar to the scale on which the Hall cascade operates in normal radio pulsars (for similar range of ages). The model with constant fields is shown to be incongruent with the data.

This rapid, nearly exponential decay effectively works – presumably – only for a relatively short period of time, and we do not expect that it is still in operation after $t \sim 10^6$ yrs.

ACKNOWLEDGEMENTS

AI thanks A.F.Kholtygin, V.A. Urpin, and K.A.Postnov for useful discussions. We are in debt to Miguel Gullón and Jose Pons, who not only provided samples for tests, but carefully read several versions of the draft of the paper and made many useful comments and suggestions during our work on this paper. We thank the unknown referee, who’s comments helped to improve the paper. We acknowledge David Jones for careful reading of the manuscript and many comments that helped to improve the text. SP thanks GGI (Florence) for hospitality during the workshop “The Structure and Sig-

nals of Neutron Stars, from Birth to Death”. SP thanks the Dynasty foundation for support of his visit to GGI. SP was supported by the RFBR grant 12-02-00186. In the middle of this research AI moved from the Saint Petersburg State University to the Radboud Universiteit Nijmegen. AI acknowledge Saint-Petersburg State University for a research grant 6.38.18.2014. AI acknowledges support from the Netherlands Research school for Astronomy (Nederlandse Onderzoekschool voor de Astronomie).

REFERENCES

- Aguilera D. N., Pons J. A., Miralles J. A., 2008, *A&A*, 486, 255
Beskin V. S., Gurevich A. V., Istomin Y. N., 1986, *Sov. Phys. Usp.*, 29, 946
Beskin V. S., Istomin Y. N., Philippov A. A., 2013, *Physics Uspekhi*, 56, 164
Bhattacharya D., Wijers R. A. M. J., Hartman J. W., Verbunt F., 1992, *A&A*, 254, 198
Boldin P. A., Popov S. B., 2010, *MNRAS*, 407, 1090
Chashkina A., Popov S. B., 2012, *New Astron.*, 17, 594
Clifton T. R., Lyne A. G., 1986, *Nature*, 320, 43
Cumming A., Arras P., Zweibel E., 2004, *ApJ*, 609, 999
Cutler C., Ushomirsky G., Link B., 2003, *ApJ*, 588, 975
Damashek M., Taylor J. H., Hulse R. A., 1978, *ApJL*, 225, L31
Deshpande A. A., Ramachandran R., Srinivasan G., 1995, *Journal of Astrophysics and Astronomy*, 16, 69
Dewey R. J., Taylor J. H., Weisberg J. M., Stokes G. H., 1985, *ApJL*, 294, L25
Eliseeva S. A., Popov S. B., Beskin V. S., 2006, arXiv:0611320
Faucher-Giguère C.-A., Kaspi V. M., 2006, *ApJ*, 643, 332
Geppert U., 2006, ArXiv Astrophysics e-prints: astro-ph/0611708
Ghosh A., Chakrabarty S., 2009, ArXiv:0911.1614
Ghosh A., Chakrabarty S., 2011, *European Physical Journal A*, 47, 56
Gonthier P. L., Ouellette M. S., Berrier J., O’Brien S., Harding A. K., 2002, *ApJ*, 565, 482
Gullón M., Miralles J. A., Viganò D., Pons J. A., 2014, ArXiv e-prints 1406.6794
Gurevich A., Beskin V., Istomin Y., 1993, *Physics of the Pulsar Magnetosphere*. Cambridge University Press
Igoshev A. P., Popov S. B., 2013, *MNRAS*, 432, 967
Igoshev A. P., Popov S. B., Turolla R., 2014, *Astronomische Nachrichten*, 335, 262
Konenkov D. Y., Popov S. B., 1997, *Astronomy Letters*, 23, 498
Lyne A. G., Lorimer D. R., 1994, *Nature*, 369, 127
Manchester R. N., Hobbs G. B., Teoh A., Hobbs M., 2005, *Astron. J.*, 129, 1993
Manchester R. N., Lyne A. G., Camilo F., Bell J. F., Kaspi V. M., D’Amico N., McKay N. P. F., Crawford F., Stairs I. H., Possenti A., Kramer M., Sheppard D. C., 2001, *MNRAS*, 328, 17
McLaughlin M. A., Stairs I. H., Kaspi V. M., Lorimer D. R., Kramer M., Lyne A. G., Manchester R. N., Camilo F., Hobbs G., Possenti A., D’Amico N., Faulkner A. J., 2003, *ApJL*, 591, L135
Ostriker J. P., Gunn J. E., 1969, *ApJ*, 157, 1395
Philippov A., Tchekhovskoy A., Li J. G., 2014, *MNRAS*, 441, 1879
Phinney E. S., Blandford R. D., 1981a, *MNRAS*, 194, 137
Phinney E. S., Blandford R. D., 1981b, *MNRAS*, 194, 137
Popov S. B., Pons J. A., Miralles J. A., Boldin P. A., Posselt B., 2010, *MNRAS*, 401, 2675

- Popov S. B., Prokhorov M. E., 2000, *A&A*, 357, 164
 Popov S. B., Prokhorov M. E., 2007, *Physics Uspekhi*, 50, 1123
 Popov S. B., Turolla R., 2012, *AP&SS*, 341, 457
 Rankin J. M., 1986, *ApJ*, 301, 901
 Sayer R. W., Nice D. J., Taylor J. H., 1997, *ApJ*, 474, 426
 Spitkovsky A., 2006, *ApJL*, 648, L51
 Thompson C., Duncan R. C., Woods P. M., Kouveliotou C., Finger M. H., van Paradijs J., 2000, *ApJ*, 543, 540
 Viganò D., Rea N., Pons J. A., Perna R., Aguilera D. N., Miralles J. A., 2013, *MNRAS*, 434, 123
 Vivekanand M., Narayan R., 1981, *Journal of Astrophysics and Astronomy*, 2, 315
 Vranešević N., Melrose D. B., 2011, *MNRAS*, 410, 2363

APPENDIX A: MATHEMATICAL PROPERTIES OF τ

A1 Averaging

Nowadays about 1700 isolated, non-millisecond pulsars are known in our Galaxy. Every pulsar can be described by a set of parameters. This set includes magnetic field, spin period, period derivative, radio luminosity, etc. Some parameters are physically related, others are independent. The spin-down age, $\tau = P/(2\dot{P})$, is the combination of the two most important and precisely measured parameters.

Let ζ be a parameter of a pulsar (it can be a spin period, magnetic field, etc.). Then the distribution function $\omega(\zeta)$ is defined as the number of pulsars in the interval from ζ to $\zeta + d\zeta$. Let it be a normalized distribution function:

$$\int_a^b \omega(\zeta) d\zeta = 1. \quad (\text{A1})$$

Averaging of some other pulsar parameter over this distribution provides an expectation value for this parameter. Individual measurements are replaced by expectation values of the same parameters everywhere in our article.

A1.1 Averaging over the initial magnetic field distribution

The initial magnetic field distribution and initial period distribution seem to be independent (Popov & Turolla 2012). Therefore, we can average over these parameters independently. Let B_0 be ζ in Eq. (A1). It is useful to use the following designation (see also Eq. 1):

$$\overline{\tau(t)}|_{B_0} = \int_{B_1}^{B_2} \tau(t, B_0') \omega(B_0') dB_0'. \quad (\text{A2})$$

Then the expression (A2) can be rewritten:

$$\overline{\tau(t)}|_{B_0} = \left. \frac{\int_0^t \beta B^2(\tau') d\tau' + 0.25 P_0^2}{\beta B^2(t)} \right|_{B_0}. \quad (\text{A3})$$

In very young neutron stars (first tens of years of their evolution), the parameter β can depend on the initial magnetic field due to star deformations (Thompson et al. 2000; Ghosh & Chakrabarty 2011, 2009; Ostriker & Gunn 1969). However, as we study much older objects, we can consider β to be independent of B_0 . We can rewrite the equation above as:

$$\overline{\tau(t)}|_{B_0} = \int_0^t \int_{B_1}^{B_2} \frac{B^2(\tau', B_0)}{B^2(t, B_0)} \omega(B_0) dB_0 d\tau' + \frac{P_0^2}{4\beta B_0^2}. \quad (\text{A4})$$

Here we assume that $B(t) = B_0 f(t)$, where $f(t)$ is a monotonic function. Thereby:

$$\overline{\tau(t)}|_{B_0} = \int_0^t \int_{B_1}^{B_2} \frac{f^2(\tau')}{f^2(t)} \omega(B_0) dB_0 d\tau' + \frac{P_0^2}{4\beta B_0^2 f^2(t)}. \quad (\text{A5})$$

We also assume that the decay function $f(t)$ does not depend on the initial magnetic field (it is related to the assumption that the function is the same for all neutron stars). The distribution function is normalized (A1), and therefore, we obtain:

$$\overline{\tau(t)}|_{B_0} = \frac{\int_0^t f^2(\tau') d\tau'}{f^2(t)} + \frac{P_0^2}{4\beta B_0^2 f^2(t)}. \quad (\text{A6})$$

This is the spin down age with a small disturbance.

A1.2 Averaging over the initial spin period distribution

Averaging over the initial spin period distribution is similar to the approach described above. First, let us consider P_0 as ζ . Similarly, we introduce the designation:

$$\overline{\tau(t)}|_{P_0} = \int_{P_1}^{P_2} \tau(t, P_0') \omega(P_0') dP_0'. \quad (\text{A7})$$

It is possible to write:

$$\overline{\tau(t)}|_{P_0} = \left. \frac{\int_0^t \beta B^2(\tau') d\tau' + 0.25 P_0^2}{\beta B^2(t)} \right|_{P_0}. \quad (\text{A8})$$

Again, in very young neutron stars β can be related to P_0 due to deformation of a rapidly rotating object (Ostriker & Gunn 1969; Cutler et al. 2003). But we can neglect it as we are dealing with older neutron stars. We write:

$$\overline{\tau(t)}|_{P_0} = \int_0^t \int_{P_1}^{P_2} \frac{B^2(\tau')}{B^2(t)} \omega(P_0) dP_0 d\tau' + \frac{P_0^2}{4\beta B^2}. \quad (\text{A9})$$

It is assumed that the initial magnetic field and spin period are independent variables. Therefore, we can write:

$$\overline{\tau(t)}|_{P_0} = \frac{\int_0^t f^2(\tau') d\tau'}{f^2(t)} + \frac{P_0^2}{4\beta B_0^2 f^2(t)}. \quad (\text{A10})$$

And again we obtain the spin down age with a small disturbance term.

A1.3 Averaging over both distributions

Now, when Eqs. (A6) and (A10) are known, we average over both parameters simultaneously:

$$\overline{\overline{\tau(t)}|_{B_0}} = \overline{\overline{\tau(t)}|_{B_0}|_{P_0}} := \overline{\tau(t)}|_{P_0, B_0}. \quad (\text{A11})$$

The result is:

$$\overline{\tau(t)}|_{P_0, B_0} = \frac{\int_0^t f^2(\tau') d\tau'}{f^2(t)} + \frac{P_0^2}{4\beta B_0^2 f^2(t)}. \quad (\text{A12})$$

APPENDIX B: ANALYTICAL DESCRIPTION OF THE ALGORITHM

In this section we use an analytical approach to describe in more detail our method of reconstruction of the decay function. This helps to demonstrate more clearly how the algorithm works without selection effects. To do this we consider several limiting cases.

B1 Distribution of initial spin-down ages

Let us define a function $\Psi(\tau_0)$ as the probability density function (PDF) of initial spin down ages τ_0 . If the PDF of the initial periods is $\Theta(P_0)dP_0$, and the PDF for the initial magnetic fields is $\Phi(\log B_0)d \log B_0$ (in the following we use notation $b = \log B_0$), then the PDF for the initial spin down ages is:

$$\Psi(\tau_0)d\tau_0 = \int_0^\infty \int_0^\infty \delta\left(\tau_0 - \frac{P_0^2}{4\beta B_0^2}\right) \Theta(P_0)\Phi(b)dP_0dbd\tau_0. \quad (\text{B1})$$

This is a sum of probabilities for all initial magnetic fields and periods which contribute to the spin down age τ_0 . Let us make a substitution $\xi = \tau_0 - P_0^2/(4\beta B_0^2)$. Then we have:

$$\begin{aligned} \Psi(\tau_0)d\tau_0 &= \int_0^\infty \Theta(P_0) \int_{-\infty}^{\tau_0} \delta(\xi) \Phi\left(\log\left[\frac{P_0}{\sqrt{4\beta(\tau_0 - \xi)}}\right]\right) \\ &\quad \times \frac{d\xi}{(\tau_0 - \xi) \ln 10} dP_0 d\xi d\tau_0. \end{aligned} \quad (\text{B2})$$

Using known properties of the delta function we can simplify this equation:

$$\Psi(\tau_0)d\tau_0 = \int_0^\infty \Theta(P_0)\Phi\left(\log\left[\frac{P_0}{\sqrt{4\beta\tau_0}}\right]\right) \frac{1}{\tau_0 \ln 10} dP_0 d\tau_0. \quad (\text{B3})$$

We assume that $\Theta(P_0)dP_0$ and $\Phi(B_0)dB_0$ are Gaussians (for the magnetic field, the distribution is in a log-scale):

$$\Theta(P_0, \mu_{P_0}, \sigma_{P_0})dP_0 = \frac{dP_0}{C_{\text{norm},1}} \exp\left(-\frac{(P_0 - \mu_{P_0})^2}{\sigma_{P_0}^2}\right), \quad (\text{B4})$$

and

$$\begin{aligned} \Phi(\log B_0, \log \mu_{B_0}, \log \sigma_{P_0})d \log B_0 &= \\ \frac{d \log B_0}{C_{\text{norm},2}} \exp\left(-\frac{(\log B_0 - \log \mu_{B_0})^2}{\log \sigma_{P_0}^2}\right). \end{aligned} \quad (\text{B5})$$

Then Eq. (B3) is expanded to:

$$\begin{aligned} \Psi(\tau_0)d\tau_0 &= \frac{d\tau_0}{C_{\text{norm}}} \int_0^\infty \exp\left(-\frac{(P_0 - \mu_{P_0})^2}{\sigma_{P_0}^2}\right) \\ &\quad \times \exp\left(-\frac{[\log(P_0/\sqrt{4\beta\tau_0}) - \log \mu_{B_0}]^2}{\log \sigma_{P_0}^2}\right) \frac{1}{\tau_0} dP_0. \end{aligned} \quad (\text{B6})$$

$$C_{\text{norm}} = C_{\text{norm},1} \times C_{\text{norm},2} \times \ln 10.$$

Next we define the fraction of pulsars born in different intervals of the average initial spin-down age:

$$C_1 = \int_0^{\bar{\tau}_0} \Psi(\tau'_0)d\tau'_0 = 0.5, \quad (\text{B7})$$

and then:

$$C_k = \int_{(k-1)\bar{\tau}_0}^{k\bar{\tau}_0} \Psi(\tau'_0)d\tau'_0. \quad (\text{B8})$$

Additionally, to interpret our results for the case of large $\bar{\tau}_0$, it is useful to introduce $C_{0.5}$:

$$C_{0.5} = \int_0^{0.5\bar{\tau}_0} \Psi(\tau'_0)d\tau'_0. \quad (\text{B9})$$

Further, we use two properties of these coefficients:

$$\sum_{k=1}^{\infty} C_k = 1, \quad (\text{B10})$$

Table B1. Coefficients C_k which describe the shape of the PDF for initial spin down ages. They are calculated numerically for $\Psi(\tau_0)$ in the form given in Eq. (B6) for representative values $\log \sigma_{B_0} = 0.5$ and $\sigma_{P_0} = 0.2$.

$C_{0.5}$	C_1	C_2	C_3	C_4	C_5	C_6
0.40	0.50	0.11	0.06	0.04	0.03	0.02
C_7	C_8	C_9	C_{10}	$\sum_{k=11}^{\infty} C_k$		
0.018	0.015	0.013	0.011	0.183		

and

$$C_{k-1} > C_k > C_{k+1}. \quad (\text{B11})$$

Results of numerical integration for the first eleven C_k are listed in the Table B1. It is worth noting that $C_{0.5}$ is rather large.

B2 Constant field and n_{br}

In this subsection we consider the case of constant magnetic field. Let us suppose that pulsars are born one by one with constant rate: each with a time step $\bar{\Delta t}$ after the previous one ($\bar{\Delta t}$ can be also considered as an average expectation time for a pulsar birth). Then C_1 is the fraction of the total number of pulsars in a considered sample born with characteristic ages $\tau_0 \leq \bar{\tau}_0$. For this group of pulsars we can write:

$$\tau(t) \leq t + \bar{\tau}_0. \quad (\text{B12})$$

For k -th group of pulsars we can write:

$$\tau(t) \leq t + k\bar{\tau}_0. \quad (\text{B13})$$

Therefore, we may use this natural expansion to represent $N(\tau)$:

$$\begin{aligned} N(\tau) &= C_{0.5} \frac{\tau - 0.5\bar{\tau}_0}{\bar{\Delta t}} + (C_1 - C_{0.5}) \frac{\tau - \bar{\tau}_0}{\bar{\Delta t}} + C_2 \frac{\tau - 2\bar{\tau}_0}{\bar{\Delta t}} \\ &\quad + C_3 \frac{\tau - 3\bar{\tau}_0}{\bar{\Delta t}} + \dots = \sum_{k=1}^{\infty} C_k \frac{\tau - k\bar{\tau}_0}{\bar{\Delta t}}. \end{aligned} \quad (\text{B14})$$

We should terminate this series when the numerator is equal to zero. Each term may be split, if necessary, into the sum of several terms as was done in Eq. (B14) for the first term. It is worth mentioning that each consecutive term is smaller than the previous one. This is obvious from Eq. (B11) and inequality $\tau - k\bar{\tau}_0 < \tau - (k+1)\bar{\tau}_0$.

As soon as we estimate the number of pulsars with the spin-down age smaller than τ , we may introduce a statistical age similar to Eq. (12):

$$T'(\tau) = \sum_{k=1}^{\infty} C_k \frac{\tau - k\bar{\tau}_0}{n_{\text{br}} \bar{\Delta t}}. \quad (\text{B15})$$

In our terminology in this example, the true birth-rate is simply $n_{\text{br}} = 1/\bar{\Delta t}$. Estimation of this quantity is one step in our method. When we perform this estimation if we fix some spin down age τ_{min} , and request that $T'(\tau_{\text{min}}) = \tau_{\text{min}}$, see Eq. (11). Then we obtain our estimate of the birthrate:

$$\tilde{n}_{\text{br}} = \sum_{k=1}^{\infty} C_k \frac{\tau_{\text{min}} - k\bar{\tau}_0}{\tau_{\text{min}} \bar{\Delta t}}. \quad (\text{B16})$$

So, in the limit $\bar{\tau}_0 \gg \tau_{\text{min}}$ we obtain that indeed $\tilde{n}_{\text{br}} = 1/\bar{\Delta t}$, i.e. here our calculated value is exact. In the case when $\tau_{\text{min}} \approx \bar{\tau}_0$

(which is a bad case), we obtain $\tilde{n}_{\text{br}} = 0.2/\sqrt{\Delta t}$. For better cases $\tau_{\text{min}} \approx 3\bar{\tau}_0$ and $\tau_{\text{min}} \approx 4\bar{\tau}_0$, we obtain $\tilde{n}_{\text{br}} = 0.37/\sqrt{\Delta t}$ and $\tilde{n}_{\text{br}} = 0.445/\sqrt{\Delta t}$, respectively. So, for realistic samples our estimate of a birthrate is between $n_{\text{br}}/5 \leq \tilde{n}_{\text{br}} \leq n_{\text{br}}$.

It is interesting to note that if we estimate \tilde{n}_{br} at $\tau_{\text{min}} \approx 3\bar{\tau}_0$, and then we restore the statistical age approximately for $5\bar{\tau}_0$, we obtain $T'(\tau) = 1.35\tau$ which means that $t > \tau$ and the field formally increases (we see it in the case of model A1, Fig. 3).

B3 Decaying field

In this subsection we consider the case of decaying magnetic field. Let us again discuss the case when pulsars are born with constant rate with separation Δt . But intervals of spin-down age between two consecutive pulsars during their evolution are not equal anymore. To perform calculations similar to the one presented in the previous subsection, we need to introduce a new function $G(\tau) = t$ and its inverse $G^{-1}(t) = \tau$. This function allows us to transform a non-uniform grid of spin-down ages τ to a uniform grid of t . The function $G^{-1}(t)$ is defined in such a way that when we substitute $G^{-1}(t)$ in the place of $\tau(t)$ into Eq. (5), then we obtain the exact function $f(t)$.² These functions $G(\tau)$ and $G^{-1}(t)$ are the inverse of each other, so $G(G^{-1}(t)) = t$ and $G^{-1}(G(\tau)) = \tau$.

To obtain an analogue of Eq. (B15) we need to have uniform time intervals in the numerator of this equation. To do this we apply our inverse function to τ in the numerator of Eq. (B15). This allows us to pass from a non-uniform grid of τ to a uniform grid of t (the true age does not depend on the magnetic field decay):

$$T'(\tau) = \sum_{k=1}^{\infty} C_k \frac{G(\tau) - k\bar{\tau}_0}{n_{\text{br}}\Delta t}. \quad (\text{B17})$$

Let us designate the result of the application of G as $t'_k = G(\tau) - k\bar{\tau}_0$. Then we apply G^{-1} to both sides of Eq. (B17):

$$\tau = G^{-1} \left(\sum_{k=1}^{\infty} C_k \frac{G(\tau) - k\bar{\tau}_0}{n_{\text{br}}\Delta t} \right). \quad (\text{B18})$$

If we substitute this τ into Eq.(5) we obtain $f(t)$:

$$f(T') = f \left(\sum_{k=1}^{\infty} C_k \frac{t'_k}{n_{\text{br}}\Delta t} \right). \quad (\text{B19})$$

Basically, in the limit $\tau \gg \bar{\tau}_0$ we have $t'_k \approx t'_1$ and $\tilde{n}_{\text{br}} = 1/\sqrt{\Delta t}$. Using properties of C_k defined by Eq. (B10) we obtain that $f(T') = f(t'_1)$.

In the limit $C_1 \approx C_2$ and $\tau_{\text{min}} \approx 2\bar{\tau}_0$ we obtain $f(T') = f(3t)$. For exponential field decay the relative error increases exponentially — $f(t)/f(3t) = \exp(2t/t_0)$, — with timescale $t_0/2$. So, in this case we obtain the decay timescale three times smaller than the actual timescale t_0 .

² Of course, technically, to define G in such a way we need to know the exact form of $f(t)$.